30

Optimal Shape of Pine for Sound Absorption in Water

H. KAWARADA [1] & H. SUITO [2]

Introduction

This paper deals with the phenomena of sound propagation near pine timber in water. A plane incident wave with frequency ω and incident angle (α, β) comes from the right hand side through medium 1(water) toward an absorbing plate made of medium 2 (pine); In fact, pine has been widely used as an absorbing material in the past.

In this case, some part of the incident wave is transmitted into the pine and the rest is reflected into the water at the surface plane.

In the first part of this paper, the problem of boundary matching is studied; in other words, the sound field of the total system is obtained using treatment of domain decomposition type. The computed domain is a rectangular parallelepiped, which is divided into two parts faced by several types of shapes.

The sound fields composed of incident and reflected waves in the water and the transmitted wave in the pine are computed separately. The total solution is obtained by coupling the two solutions computed in each domain to satisfy transmission conditions defined on an interfacial boundary. Here, let us construct the cost function of a Dirichlet-Neumann type on the boundary, which is directly minimized by means of Fuzzy Optimization Method (FOM)[KOPS98, KS97].

In order to evaluate the shape of the interfacial boundary in pursuit of a better absorption of the sound field into the pine, we proceed to the second part; i.e., shape optimization. We denote the flat interfacial boundary by Γ_0 and expect that

1 Faculty of engineering, Chiba University, Inage-ku, Chiba, 263-8522, JAPAN. email: kawarada@applmath.tg.chiba-u.ac.jp
2 Address same as above. email: suito@applmath.tg.chiba-u.ac.jp
Eleventh International Conference on Domain Decomposition Methods
Editors Choi-Hong Lai, Petter E. Bjørstad, Mark Cross and Olof B. Widlund ©1999 DDM.org

an appropriate Γ deformed from Γ_0 brings about the increase of the amplitude of the transmitted wave into pine. The minimization problem, the cost of which is represented by the amplitude defined on the fixed flat surface in the pine, is proposed with Γ regarded as a control variable. Here, the deformation of Γ is represented by a superposition of the product of two scaling functions for a wavelet. The admissible set due to this choice seems to be considerably restricted, but the merit of this use is an appearance of wedge-shaped patterns involved in them, which have been used as the shape of absorption materials for a long time. Finally, the minimization problem constructed is also directly solved by means of FOM.

The reason why we have not used elegant techniques developed in the framework of domain decomposition is due to the requirement to test the validity and the utility of direct minimization by use of FOM. At the present stage we have confirmed the numerical solvability of the problems, but cannot discuss the suitability of this strategy without comparison with various othrt methods approached from a range of viewpoints.

The algorithm to solve the minimization problems numerically is divided into two parts;

1. 2D/3D Helmholtz solver for deformed region;
   Here we solve the Helmholtz equation in the deformed region by the use of finite difference approximation. The mesh generation method of an elliptic type is effectively adopted and also the GPBi-CG method[Zha97] is used to solve a discretized Helmholtz equation defined in the computed domain, where the preconditioning technique causes a surprising effect to save an iteration number.
2. Fuzzy Optimization Method;
   This is used to solve the minimization problem. This method is briefly reviewed in this paper.

The contents of this paper are as follows; 1. Introduction, 2. Applications, 3. Deformation of the interfacial boundary, 4. Shape optimization, 5. Numerical Solution of Helmholtz Eq., 6. Hybrid Algorithm by FOM and GAs, 7. Numerical Results, 8. Conclusions.

Applications

Optimal shape design problems for;

1. Anti-noise wall for high-speed trains (Shinkansen) running through densely populated areas,
2. Sonar domes at the bows or bottom of a ship,
3. Input surface of a solar battery,
4. Noise absorption for engine rooms,
5. Etc,

could be treated in almost the same framework as that introduced in this paper.

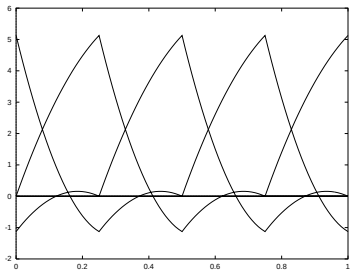

Figure 1 Scaling functions

Deformation of the Interfacial Boundary

Scaling functions for wavelet

Wedge-shaped patterns often arise in wavelets. A scaling function for wavelets is introduced as follows;
Let

$$\eta_0(x) = \begin{cases} 1 & x \in [0,1], \\ 0 & else, \end{cases} \tag{1}$$

and

$$\begin{aligned} f_0(x) &= (-0.585x^2 + 1.867x)\eta_0(x), & (2)\\ f_1(x) &= (1.170x^2 - 2.734x + 1.282)\eta_0(x), & (3)\\ f_2(x) &= (0.585x^2 + 0.867x - 0.282)\eta_0(x). & (4) \end{aligned}$$

Then

$$\phi(x) = f_0(x) + f_1(x-1) + f_2(x-2) \tag{5}$$

satisfies

1. supp $\phi = [0,3]$
2. $\displaystyle\int_R \phi(x)dx = 1$
3. An auto-correlation function $\phi^{[2]}(x) = \int_R \phi(x+y)\phi(y)dy$ satisfies $\phi^{[2]}(m) = \delta_{m,0} \ \ (m \in Z)$.

Define

$$\phi_{L,m}(x) = \sqrt{N_L} \cdot \phi(N_L x - m) \ \ (m \in Z) \tag{6}$$

where $N_L = 2^L$.

Then $\{\phi_{L,m}\}$ constitutes an orthonormal set, i.e.,

$$\int_R \phi_{L,m}\phi_{L,m'}dx = \delta_{m,m'}. \tag{7}$$

Figure 1 shows an example of $y = \phi_{L,m}(x)$, where $L = 2$ and $m = 1, 2, \cdots, 6$.

Admissible Set for the Deformed Surface

Represent the deformed surface by means of a superposition of $\phi_{L,m}(y)\phi_{L,m'}(z)$, i.e.,

$$\Gamma = \sum_{m,m'} \gamma_{mm'} \cdot \phi_{L,m}(y)\phi_{L,m'}(z). \tag{8}$$

The admissible set for the deformation of the interfacial boundary is defined by

$$\mathcal{A}_1 = \{\gamma_{mm'} \in R | \, |\gamma_{mm'}| \leq K \ (m, m' = 1, 2, 3, \cdots, M_1)\}. \tag{9}$$

Shape optimization

Configuration

- $\Gamma_{top}, \Gamma_{side}$ and Γ_{bottom} are rigid boundaries, i.e., the density of these walls is infinite. Hence, sound waves are entirely reflected at these boundaries.
- Γ_{in} is a vibrating plate which makes sound wave.
- Ω_1 is occupied by water.
- Ω_2 is made of pine, the role of which is to absorb the sound wave coming through Ω_1.
- Γ is the boundary between Ω_1 and Ω_2. We will try to optimize its shape to absorb the sound wave into Ω_2 as completely as possible.
- Ω_3 is a so-called Fictitious Domain, i.e., an artificial domain to approximate the boundary condition at infinity. In this domain, the Helmholtz eq. with a complex wave number is assumed, which is derived from Navier-Stokes eq. including a viscosity term. A sound wave transmitted from Ω_2 is almost completely damped in this domain and is not reflected into Ω_2.
- Γ_{absorb}, on which the amplitude of the absorbed sound wave in Ω_2 is computed.
- Γ_{out}, on which the sound wave does not exist because of the damping effect in the domain Ω_3.
- $\Omega = \Omega_1 \cup \Gamma \cup \Omega_2 \cup \Omega_3 = (0, l_x) \times (0, l_y) \times (0, l_z)$
- $u^{(i)}(x, y, z)$ $(i = 1, 2, 3)$: Complex sound pressure.
- k_i $(i = 1, 2, 3)$: Wave number.
- λ_i $(i = 1, 2, 3)$: Wave length.
- c_i $(i = 1, 2, 3)$: Sound speed.
- ω : Angular velocity of the incident wave.

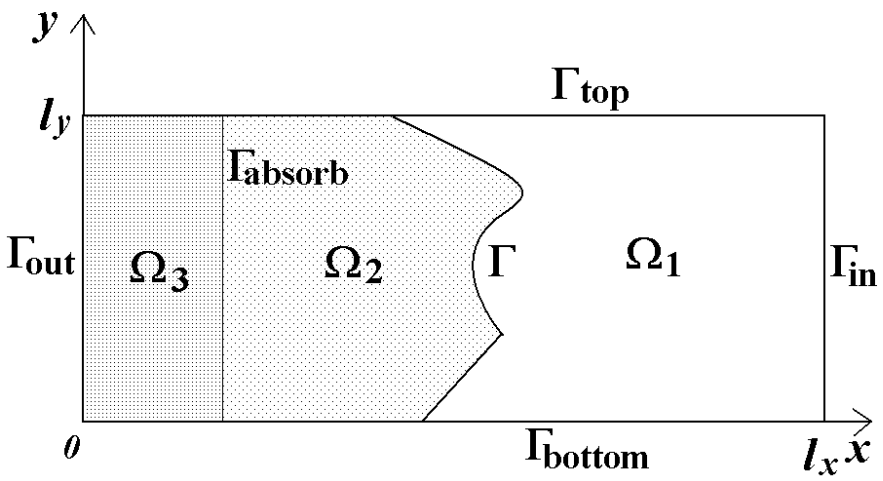

Figure 2 Projection of computed domain into $x-y$ plane

- ρ_i $(i = 1, 2, 3)$: Density of medium.
- $\mathbf{n}$: Outward normal vector on the boundaries.
- Γ : Interfacial boundary between Ω_1 and Ω_2.
- α, β : An incident angle of plane wave,

where $i = 1$ means water, $i = 2$ means pine and $i = 3$ means the fictitious domain.

Physical data

Table 30 shows the physical data of media used in our problem.

Minimization with the Constraint

Define the state equation;

$$\begin{cases} (\triangle + k_i^2)\, u^{(i)}(\Gamma, a) = 0 & \text{in } \Omega_i, \quad (i = 1, 2, 3), \\ u^{(1)}(\Gamma, a) = u^{(2)}(\Gamma, a) = a & \text{on } \Gamma, \\ \dfrac{\partial u^{(i)}(\Gamma, a)}{\partial n} = 0 & \text{on } \Gamma_{top} \cup \Gamma_{bottom}, \\ & \quad \cup \Gamma_{side} (i = 1, 2, 3), \\ u^{(1)}(\Gamma, a) = e^{ik_1 \cos\beta l_x} e^{ik_1 \sin\beta \cos\alpha y} e^{ik_1 \sin\beta \cos\alpha z} & \text{on } \Gamma_{in}, \\ u^{(2)}(\Gamma, a) = 0 & \text{on } \Gamma_{out}, \end{cases} \tag{10}$$

and the cost function;

Table 1 Physical data of media

	Water	Pine
$\rho\ (kg/m^3)$	998.9	450.0
$k\ (rad/m)$	53.51	25.5
$\lambda\ (m)$	0.12	0.25
$c\ (m/sec)$	1467.8	3599.4
$\omega\ (rad/sec)$	7.85×10^4	7.85×10^4

$$J_c(\Gamma, a) = -\int_{\Gamma_{absorb}} \left| u^{(2)}(\Gamma, a) \right|^2 d\Gamma$$
$$+\frac{1}{\varepsilon}\int_{\Gamma} \left| \frac{1}{\rho_1}\frac{\partial u^{(1)}(\Gamma, a)}{\partial n} - \frac{1}{\rho_2}\frac{\partial u^{(2)}(\Gamma, a)}{\partial n} \right|^2 d\Gamma, \quad (\varepsilon > 0). \tag{11}$$

The Dirichlet datum a is defined on Γ by

$$a = \sum_{mm'} a_{mm'} \cos(\frac{\pi m}{l_y} y) \cos(\frac{\pi m'}{l_z} z). \tag{12}$$

A The admissible set for a is represented by

$$\mathcal{A}_2 = \{a_{mm'} \in \mathbf{C} \ \ (m, m' = 0, 1, 2, \cdots, M_2) || a_{mm'}| \leq L\}. \tag{13}$$

The minimization problem is;

$$[Pr_c]: \quad \text{Minimize} J_c(\Gamma, a) \ \text{ for } \ (\Gamma, a) \in \mathcal{A} = \mathcal{A}_1 \times \mathcal{A}_2.$$

Numerical Solution of Helmholtz Eq. in the Deformed Region

In order to compute the sound field in a domain with a complicated boundary, the following coordinate transformation is used;

1. Generate a mesh system in the deformed domain, which is the transformation from a physical domain to a computational one;

$$\begin{aligned} x &= x(\xi, \eta, \zeta), \\ y &= y(\xi, \eta, \zeta), \\ z &= z(\xi, \eta, \zeta). \end{aligned} \tag{14}$$

2. Transform differential operators by use of (14).
3. Transform Helmholtz eq. by use of (14).

Discretized Helmholtz Eq. in the Computational Domain

Helmholtz equation in the physical domain;

$$(\partial_{xx} + \partial_{yy} + \partial_{zz})u + k^2 u = 0, \tag{15}$$

is written in the computational domain as follows;

$$\begin{aligned}
&\Big(\frac{a_{11}}{J}\partial_\xi(\frac{a_{11}}{J}\partial_\xi + \frac{a_{12}}{J}\partial_\eta + \frac{a_{13}}{J}\partial_\zeta) + \frac{a_{12}}{J}\partial_\eta(\frac{a_{11}}{J}\partial_\xi + \frac{a_{12}}{J}\partial_\eta + \frac{a_{13}}{J}\partial_\zeta)\\
&+\frac{a_{13}}{J}\partial_\zeta(\frac{a_{11}}{J}\partial_\xi + \frac{a_{12}}{J}\partial_\eta + \frac{a_{13}}{J}\partial_\zeta) + \frac{a_{21}}{J}\partial_\xi(\frac{a_{21}}{J}\partial_\xi + \frac{a_{22}}{J}\partial_\eta + \frac{a_{23}}{J}\partial_\zeta)\\
&+\frac{a_{22}}{J}\partial_\eta(\frac{a_{21}}{J}\partial_\xi + \frac{a_{22}}{J}\partial_\eta + \frac{a_{23}}{J}\partial_\zeta) + \frac{a_{23}}{J}\partial_\zeta(\frac{a_{21}}{J}\partial_\xi + \frac{a_{22}}{J}\partial_\eta + \frac{a_{23}}{J}\partial_\zeta)\\
&+\frac{a_{31}}{J}\partial_\xi(\frac{a_{31}}{J}\partial_\xi + \frac{a_{32}}{J}\partial_\eta + \frac{a_{33}}{J}\partial_\zeta) + \frac{a_{32}}{J}\partial_\eta(\frac{a_{31}}{J}\partial_\xi + \frac{a_{32}}{J}\partial_\eta + \frac{a_{33}}{J}\partial_\zeta)\\
&+\frac{a_{33}}{J}\partial_\zeta(\frac{a_{31}}{J}\partial_\xi + \frac{a_{32}}{J}\partial_\eta + \frac{a_{33}}{J}\partial_\zeta)\Big)\, u + k^2 u = 0
\end{aligned} \tag{16}$$

where

$$a_{11} = y_\eta z_\zeta - y_\zeta z_\eta,\ a_{12} = y_\zeta z_\xi - y_\xi z_\zeta,\ a_{13} = y_\xi z_\eta - y_\eta z_\xi, \tag{17}$$

$$a_{21} = z_\eta x_\zeta - x_\eta z_\zeta,\ a_{22} = x_\xi z_\zeta - x_\zeta z_\xi,\ a_{23} = x_\eta z_\xi - x_\xi z_\eta, \tag{18}$$

$$a_{31} = x_\eta y_\zeta - y_\eta x_\zeta,\ a_{32} = y_\xi x_\zeta - x_\xi y_\zeta,\ a_{33} = x_\xi y_\eta - y_\xi x_\eta, \tag{19}$$

$$J = \begin{vmatrix} x_\xi & x_\eta & x_\zeta \\ y_\xi & y_\eta & y_\zeta \\ z_\xi & z_\eta & z_\zeta \end{vmatrix}. \tag{20}$$

The boundary conditions defined on the boundaries of the physical domain are each transformed in a similar way. (16) is discretized by second order central differences.

Mesh Generation of an Elliptic Type

In order to generate a smooth mesh structure along the deformed boundary, an elliptic type of mesh generation method is adopted. In this method, the following three Laplace equations are solved in the computational domain;

$$\xi_{xx} + \xi_{yy} + \xi_{zz} = 0, \tag{21}$$

$$\eta_{xx} + \eta_{yy} + \eta_{zz} = 0, \tag{22}$$

$$\zeta_{xx} + \zeta_{yy} + \zeta_{zz} = 0, \tag{23}$$

where $\xi = \xi(x, y, z), \eta = \eta(x, y, z)$ and $\zeta = \zeta(x, y, z)$.

The numbers of mesh points along ξ, η and ζ directions are 161, 21 and 21, respectively.

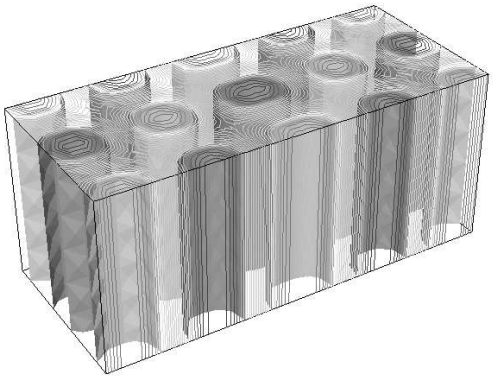

Figure 3 Exact solution

Algorithm to Solve the Discretized Helmholtz Eq.

The discretized Helmholtz eq. for (16) constitutes a large scale of linear system of equations. In order to solve this system of equations, GPBi-CG method[Zha97] is adopted.

Furthermore, in order to validate our Helmholtz solver, we compare numerical solutions with an exact solution;

$$\begin{aligned} u &= \exp(ik\cos\beta x)\exp(ik\sin\beta y) \\ &+ \exp(ik\cos\beta x)\exp(-ik\sin\beta y) \\ &= 2\exp(ik\cos\beta x)\cos(k\sin\beta y). \end{aligned} \tag{24}$$

Figure 3 shows the iso-surfaces of a real part of the exact solution.

Figures 4 and 5 show iso-surfaces of a real part of the numerical solution and some grid lines in the cases where the interfacial boundary Γ is flat and deformed, respectively.

In both cases, a good agreement between the numerical solutions and the exact solution is obtained. And it guarantees that our Helmholtz solver is reasonably reliable.

The CPU time needed to solve once Helmholtz eq. is approximately 20 seconds by DEC Alpha 533MHz.

Hybrid Algorithm by FOM and GAs

In this section, Fuzzy optimization Method (FOM) is briefly summarized.

1. Fuzzy Optimization Method[KS97]
   Modification of the steepest descent method by means of stochastic Fuzzy ruling.

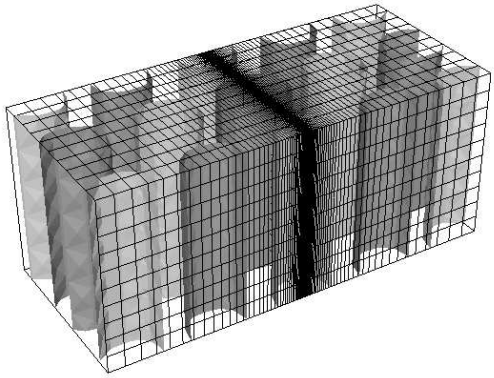

Figure 4 Numerical solution by orthogonal mesh

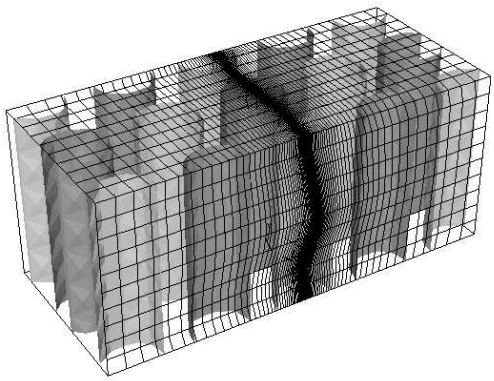

Figure 5 Numerical solution by boundary fitting mesh

2. Single-start FOM[KS97]
   Combination of FOM and Mountain Crossing Algorithm (MCA).
3. Multi-start FOM[KOPS98]
   An increase of the number of initial points. Let operators F, M and R be defined as follows;

   - F : Algorithm due to single-start Fuzzy optimization method,
   - M : Mountain crossing algorithm,
   - R : Rearrangement algorithm by GAs.

   Then the algorithm of Multi-start FOM is stated in the following way;

   (a) Give an initial population W^0 (the set of patrols).
   (b) Compute $U^n := FW^n$ (the set of local minimizers obtained).
   (c) Compute $V^n := MU^n$ (the set of quasi-local maximizers obtained).
   (d) Compute $W^n := RV^n$ (the set of rearranged patrols).
   (e) Increase the generation number $n := n + 1$ and repeat the steps from (b) to (d) until the generation number n is beyond the preset one.

4. Hierarchical Multi-start FOM (To be published)

   (a) Decompose the searching domain into an appropriate number of sub-domains.
   (b) Search local minimizers by Multi-start FOM in each sub-domain.
   (c) Rearrange the sub-domains by GAs or Multi-start FOM.
   (d) Increase the generation number $n := n + 1$ and repeat steps (b) and (c) until the generation number n is beyond the preset one.

Numerical Results

An incident angle is chosen ($\alpha = 0, \beta = 30(> \beta_c)$) in all cases. β_c is a critical angle at which the complete reflection occurs in the case of a flat interfacial boundary;

$$\sin \beta_c = \frac{k_2}{k_1}. \tag{25}$$

First, the boundary matching problem is considered. In this case, the interfacial boundary is flat and the cost function is defined as follows;

$$J_b(a) = \int_\Gamma \left| \frac{1}{\rho_1} \frac{\partial u^{(1)}(a)}{\partial n} - \frac{1}{\rho_2} \frac{\partial u^{(2)}(a)}{\partial n} \right|^2 d\Gamma. \tag{26}$$

Figure 6 shows the absolute value of complex sound pressure after the optimization process terminates.

Since incident angle β is larger than the critical angle β_c, numerical results show that a sound wave is almost completely reflected into the water region.

We then optimize the shape of the interfacial boundary under the constraint of the matching of transmission condition, i.e., Shape Optimization Problem. Figure 7

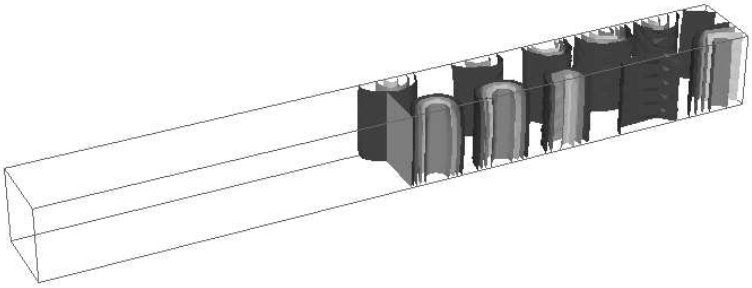

Figure 6 Boundary matching problem (absolute value)

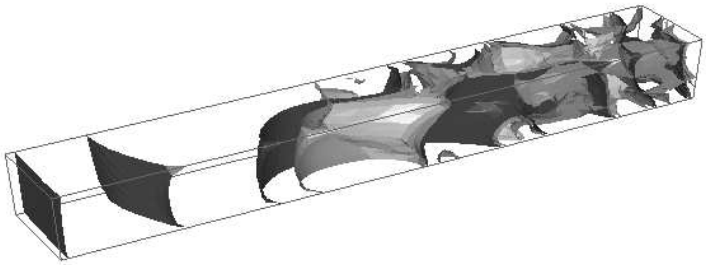

Figure 7 Shape optimization (absolute value)

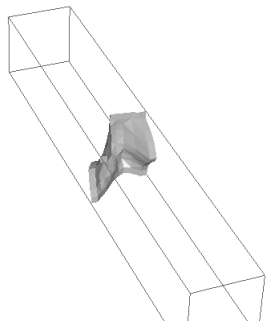

Figure 8 Optimal shape of the interfacial boundary Γ

shows the absolute value of complex sound pressure after the optimization process terminates.

As a result of shape optimization of the interfacial boundary, numerical results show that a large portion of the sound wave is transmitted into the pine region.

Figure 8 shows the optimal shape of interfacial boundary Γ after the 15th iteration.

Conclusions

Carrying out the computations in this paper, one of the difficulties we had to overcome was to construct a 2D/3D Helmholtz solver in the deformed region. The technique of preconditioning in iteration contributed much to solving large scale discretized equations. The description of variation in the usual application of shape design techniques was not adopted here, i.e., it means there was no use of the variation distributed on the lattice points. The deformation of interfacial boundary is represented by a superposition of the scaling functions in wavelets, that make it not only easy to compute the deformed boundary in each iterative step of the optimization, but also encapsulates the nature of the present problem. The use of FOM as the minimization technique demonstrated its validity and utility by producing satisfactory numerical results. Thanks to the combined use of the above-mentioned techniques, it seems that reasonable results can be obtained from a numerical point of view.

REFERENCES

[KOPS98] Kawarada H., Ohtomo T., Periaux J., and Suito H. (1998) Multi-start fuzzy optimization method. In *GAKUTO International Series, Mathematical Sciences and Applications, Vol. 11*, pages 338–345. Gakko Tosho, Tokyo, Japan.

[KS97] Kawarada H. and Suito H. (1997) Fuzzy optimization method. In *Computational Science for the 21th Century*, pages 642–651. John Wiley & Sons.

[Zha97] Zhang S.-L. (1997) GPBi-CG : Generalized product-type methods based on bi-cg for solving nonsymm *SIAM J. on Scientific Computing* 18-2: 537–551.